Pharmaceutical Research, Vol. 22, No. 10, October 2005 (© 2005)
DOI: 10.1007/s11095-005-6947-z

Research Paper

Mechanism of the Solution Oxidation of Rofecoxib Under Alkaline Conditions

Paul A. Harmon,[1,3] Stephen Biffar,[1] Steven M. Pitzenberger,[2] and Robert A. Reed[1]

Received February 16, 2005; accepted June 23, 2005

Purpose. The rapid oxidation of rofecoxib under alkaline conditions has been previously reported. The oxidation was reported to involve γ-lactone ring opening to an alcohol, which further oxidized to a dicarboxyclic acid. The oxidation was suspected to be mediated by peroxy radicals. This work further investigates the mechanism of oxidation under the alkaline solution conditions.
Methods. The pH dependence of the oxidation reaction was determined in 50% acetonitrile/50% aqueous phosphate buffer (pH 9–12). The oxidation reaction products were also examined at early timepoints (from 40 s to several minutes) with only 5% water content. The evolution of hydrogen peroxide by the oxidation reaction was quantitatively followed by reaction with triphenylphosphine (TPP) and high-pressure liquid chromatography determination of the resultant triphenylphosphine oxide formed. Rofecoxib was exposed to the alkaline pH conditions in the presence of formaldehyde, and the primary reaction product was isolated and characterized by liquid chromatography-mass spectrometry and proton 1D, heteronuclear multiple quantum coherence (HMQC), gradient heteronuclear multiple bond correlation (gHMBC), and carbon 1D nuclear magnetic resonance techniques. Transient reaction products were examined for hydroperoxide groups by reaction with TPP.
Results. The oxidation reaction occurs only near pH 11 and above. In the presence of excess formaldehyde, oxidation products are no longer observed but a new product is observed in which two formaldehyde molecules have added to the methylene carbon atom of the γ-lactone ring. The evolution of hydrogen peroxide corresponds quantitatively to the molar amount of the (minor) aldehyde oxidation product formed. It is demonstrated that the rofecoxib anhydride species is actually the primary product of the oxidation reaction. The existence of a transient hydroperoxide species is shown by reaction with TPP and concomitant conversion to a previously identified alcohol.
Conclusions. The oxidation of rofecoxib under these high pH conditions is mediated by rofecoxib enolate ion formation. The enolate ion reacts with either formaldehyde or dissolved oxygen at the C_5 position. In the case of oxygen, a transient hydroperoxide species is formed. The major and minor products of the oxidation derive from competitive routes of decomposition of this hydroperoxide. The major route involves a second enolate ion formation, which decomposes with heterolytic cleavage of the RO–OH bond to give the rofeocoxib anhydride and hydroxide ion. The anhydride is rapidly hydrolyzed under the alkaline conditions to give the observed rofecoxib dicarboxylate product. The minor hydroxyfuranone product is formed from hydroxide ion attack on the hydroperoxide intermediate.

KEY WORDS: base-catalyzed; enolate ion; mechanism; oxidation; rofecoxib; stability.

INTRODUCTION

During early development of an active pharmaceutical ingredient, it may become evident that oxidation of the compound is an issue. In such cases, achieving a complete mechanistic understanding of the relevant oxidative degradation pathways poses a considerable challenge for the pharmaceutical scientist. The challenge derives from the potential complexity and types of oxidative degradation mechanisms possible, which have been reviewed (1–3). Oxidative decomposition of pharmaceuticals involving the formation of new carbon–oxygen bonds often involves free radical chain processes. These reactions require initiation events that may involve heat, light, or metal ions. Formation of N oxides and sulfoxide degradates often involves direct "two-electron" reactions of the sulfur and nitrogen atoms with trace levels of hydroperoxides and thus may not involve free radicals (1,4,5). Base catalyzed oxidation (2,6) and oxidation by singlet oxygen have also been reported (7,8). A mechanistic understanding of the operating oxidative pathway at hand is important as it facilitates the intelligent design of appropriate inhibition strategies. A thorough understanding of the potential oxidative processes is thus of fun-

[1] Department of Pharmaceutical Analysis and Control, Merck Research Laboratories, P.O. Box 4, West Point, Pennsylvania 19486, USA.
[2] Department of Medicinal Chemistry, Merck Research Laboratories, P.O. Box 4, West Point, Pennsylvania 19486, USA.
[3] To whom correspondence should be addressed. (e-mail: Paul_Harmon@Merck.com)

damental importance. It is in this context that we became interested in the mechanism of the rapid oxidation of rofecoxib under alkaline pH conditions as reported by Mao *et al.* (9) in 2002.

The oxidation previously reported is shown in Scheme 1 (adapted from Mao *et al.*). Although the authors focused largely on determining the structure of the oxidation products, the need for both oxygen and high pH conditions was demonstrated. A general mechanism for the oxidation was suggested which required an initial opening of the rofecoxib γ-lactone ring; this is shown in Scheme 1.

Ring opening produces the alcohol (**2**) that the authors speculate undergoes air oxidation to hydroxy-furanone (**3**) (minor product) and dicarboxyclic acid (**4**) (major product). Oxidation from the alcohol to the hydroxy-furanone (**3**) and further to the dicarboxylic acid was noted to be consistent with free radical chain oxidation mediated by peroxy radicals, $ROO^{\bullet}$ (1–3).

We agree with Mao *et al.* that peroxy radicals mediate most oxidative degradation processes observed in pharmaceutical dosage forms and solutions. However, peroxy radical oxidation is relatively slow due to the rate limiting step of hydrogen atom abstraction by the peroxy radical (1–3). Oxidation of the alcohol (**2**) to the carboxylic acid (**4**) by peroxy radicals would require two C–H bond hydrogen atom abstractions. Our laboratory has investigated simple peroxy radical model systems and has examined relative reaction rates of numerous drug substance C–H bonds with peroxy radicals (P. A. Harmon, K. Kosuda, E. Nelson, M. Mowery, and R. A. Reed, A novel peroxy radical based oxidative stressing system, manuscript in review). The rofecoxib oxidation reported by Mao *et al.* seems to proceed nearly 2 orders of magnitude faster than any C–H bond abstraction we have seen in our peroxy radical model systems. Given this unusually rapid reaction rate, as well as lack of obvious source of peroxy radicals under the rofecoxib reaction conditions, this work attempts to elucidate the mechanistic details of the oxidation shown in Scheme 1.

MATERIALS AND METHODS

Materials

High-pressure liquid chromatography (HPLC)-grade solvents were obtained from Sigma-Aldrich (St. Louis, MO, USA). triphenylphosphine (TPP, 99%) and triphenylphosphine oxide (TPO, 99%) were obtained from ACROS Organics Corporation (Geel, Belgium). Formaldehyde (37%) was obtained from Sigma. Deuterated acetonitrile (99.96 at.% D) for the nuclear magnetic resonance (NMR) characterization was obtained from Cambridge Isotope Labs (Andover, MA, USA). Tetramethylsilane (TMS) was obtained from Sigma-Aldrich. Rofecoxib was supplied by Merck (Rahway, NJ, USA).

Methods

Alkaline pH Oxidation of Rofecoxib and Monitoring by HPLC

The alkaline oxidation experiments were carried out in 50% acetonitrile/50% 20 mM phosphate buffer at pH 11.0 or 12.0 as noted below. Three milliliters of a 0.1 or a 0.2 mg/mL solution of rofecoxib in 100% acetonitrile was mixed with 3 mL of the alkaline phosphate buffer to initiate the reaction; the 6-mL reaction mixture was stirred in a closed system with 15 mL of headspace. At each timepoint, an HPLC vial was filled and the sample injected immediately. The experiments in which the aqueous content was varied were carried out in HPLC vials by appropriate volumetric addition of phosphate buffer to a known volume of rofecoxib in 100% acetonitrile. The reactions in the presence of formaldehyde were also done similarly in HPLC vials by volumetric addition of 37% formaldehyde or dilutions thereof. The reaction mixtures were injected directly without any neutralization unless otherwise noted.

An Agilent 1100 series HPLC equipped with a quaternary pump, vacuum degasser, diode array detector and

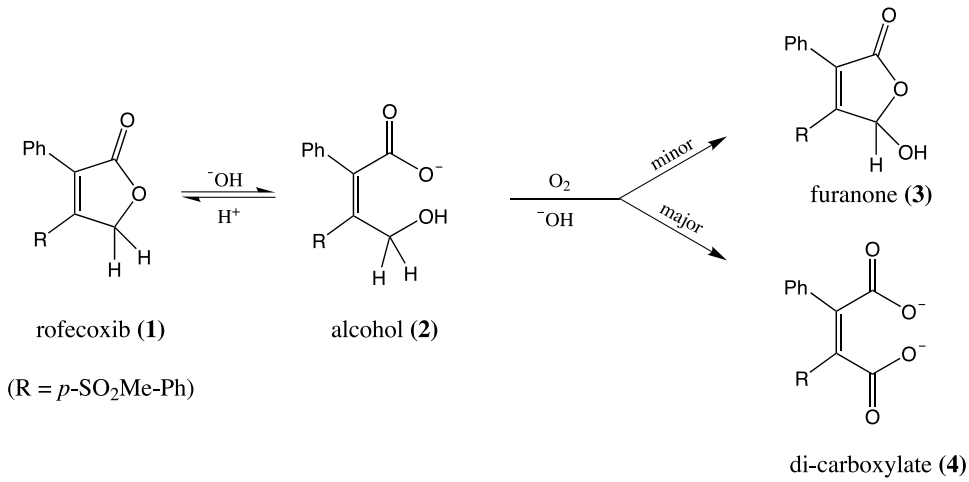

Scheme 1. General mechanism for rofecoxib oxidation at high pH from Mao *et al.* (9).

autosampler (at ambient temperature) (Agilent Technologies, USA) was utilized. The chromatographic conditions were taken from Mao *et al.* (9) and modified for our purposes. The chromatographic conditions used were as follows: column, Waters Symmetry C18 (15 cm×3.9 mm, 5 μm packing); column temperature, 40°C; flow rate, 1.5 mL/min; injection volume, 5 μL; detection wavelength, 220 nm. The mobile phase components were acetonitrile and 10 mM phosphate buffer ($NaH_2PO_4 \cdot H_2O$) at an ambient pH of 4.6. The linear gradient conditions were as follows: at initial, 75% phosphate buffer, 25% acetonitrile, to 70% phosphate, 30% acetonitrile over 4 min; then to 49% phosphate buffer, 51% acetonitrile over the next 9 min. The mobile phase composition was then returned to the initial conditions over a 1.0-min period and reequilibrated for 5 min.

Determination of Liberated Hydrogen Peroxide Using TPP

Triphenylphosphine (TPP) was used for determining the hydrogen peroxide or organic hydroperoxide (ROOH) content of solutions. A 2.0-mL portion of the oxidation reaction solution was taken as a function of time and quenched with 2.0 mL of a 50% acetonitrile/50% 20 mM phosphate (pH 2.3) solution. A 1.0-mL portion of the quenched sample solution was then added to a 4.0-mL aliquot of a TPP stock solution. The TPP stock solution was 0.10 mg/mL TPP in 100% methanol. The sample was then allowed to react for 15 min. The amount of triphenylphosphine oxide (TPO) formed by the reaction of hydrogen peroxide with the TPP was then determined by HPLC. Chromatographic conditions: column, 5 cm×4.6 mm Synergi Polar-RP; column temperature, 40°C; flow rate, 1.0 mL/min; injection volume, 10 μL; detection wavelength, 203 nm; and an isocratic mobile phase composition of 75% methanol/25% water. Rofecoxib eluted at 1.4 min and was resolved from TPO which eluted near 1.8 min, whereas TPP eluted near 6.0 min. The concentration (mol/L) of the TPO present was determined by injection of a bracketing TPP standard solution of 0.08 mg/mL.

LC-MS Analysis of Oxidation Products and Formaldehyde Adducts

For liquid chromatography-mass spectrometry (LC-MS), the HPLC conditions were identical to that describe above except for a change in the mobile phase components to acetonitrile and 0.01% formic acid and a slight alteration of the gradient profile: at initial, 75% 0.01% formic acid/ 25% acetonitrile, to 70% 0.01% formic acid, 30% acetonitrile over 4 min; then to 45% 0.01% formic acid, 55% acetonitrile over the next 11 min. The mobile phase composition was then restored to the initial conditions over a 1.0-min period and reequilibrated for 5 min. An Agilent 1100 series HPLC (identical to that described above) sourced the MS instrument.

The alkaline samples were quenched with acid prior to injection for the LC-MS experiments. A Thermo-Finnegan LCQ Deca XP Plus MS system was used with APCI ionization and positive ion mode detection. The capillary temperature was 250°C, and the APCI vaporizer temperature was 450°C. The source voltage and current were 4.5 kV and 5.0 μA, respectively.

Isolation of bis-Formaldehyde Adduct of Rofecoxib for NMR Analysis

A solution of Rofecoxib at 3 mg/mL in 50% acetonitrile/50% phosphate buffer (pH 12.0) was prepared in the presence of a threefold molar excess of formaldehyde and allowed to react for 10 min. Five 100-μL injections of this solution were made and the bis-formaldehyde species fractionated, giving about 1 mg of product. For the fractionation, the HPLC conditions were as follows: column, 25 cm×4.6 mm Waters X-Terra C18; column temperature, 40°C; isocratic mobile phase consisting of 75% water and 25% acetonitrile. Solvent was removed by rotoevaporation using vacuum and an ambient temperature water bath.

NMR Analysis of bis-Formaldehyde Adduct of Rofecoxib

The ~1 mg of the bis-formaldehyde product was dissolved in 0.65 mL CD_3CN. Tetramethylsilane was added as an internal chemical shift reference. Proton 1D, heteronuclear multiple quantum coherence (HMQC), and gradient heteronuclear multiple bond correlation (gHMBC) spectra were recorded using standard pulse sequences on a Varian Unity Inova 600 NMR spectrometer equipped with a triple resonance indirect detection probe (HCN). An ^{1}H-decoupled ^{13}C-observe spectrum was acquired on a Varian Unity Inova 500 NMR spectrometer equipped with a CHF triple resonance probe. The sample temperature was held at 25°C.

RESULTS

Time Evolution and pH Dependence of the Rofecoxib Oxidation

Figure 1 shows an overlay of chromatograms from the oxidation of 0.1 mg/mL rofecoxib in 50% acetontrile/50% 20 mM phosphate buffer (pH 11.0). Relative yields, relative retention times, and LC-MS data confirm that the major product species eluting near 0.8 min is the dicarboxyclic acid **4**, whereas the minor product eluting near 6.1 min is the hydroxy-furanone **3**, as reported by Mao *et al.* Figure 2 plots the loss of rofecoxib peak area and concomitant gain in peak area of the major and minor products over a 4-h period.

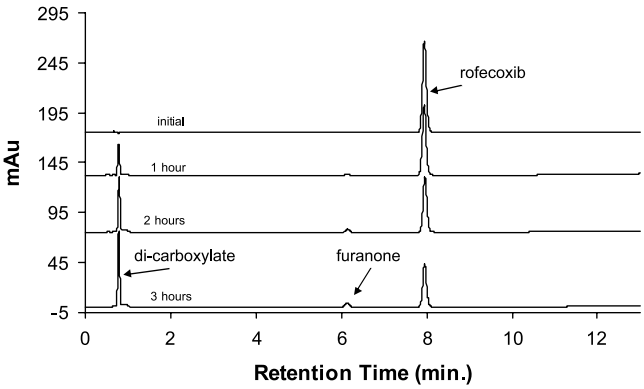

Fig. 1. Direct injections of rofecoxib oxidation reaction (50% acetonitrile/50% phosphate buffer, pH 11.0) as a function of time. Initial, 1, 2, and 3 h (top to bottom). Major product is early eluting dicarboxylate (**4**) with minor furanone product (**3**) near 6.1 min.

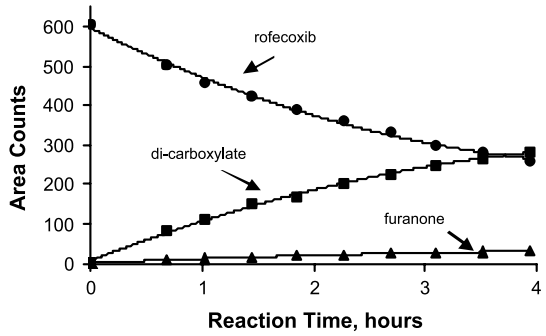

Fig. 2. Plot of peak area of rofecoxib (**1**) (circles), dicarboxylate (**4**) (squares), and furanone (**3**) (triangles) over 4 h reaction time. Conditions as in Fig. 1.

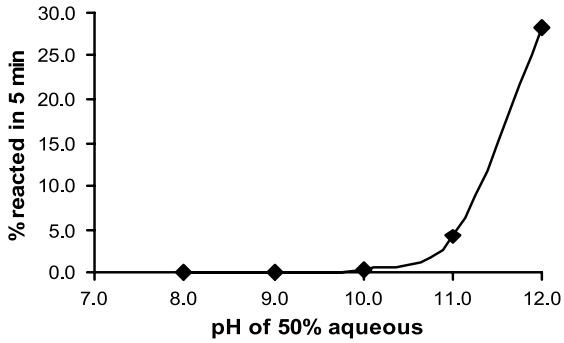

Fig. 3. Plot of percentage rofecoxib (**1**) reacted during the first 5 min of reaction time *vs.* the pH of the 50% aqueous component of the reaction mixture.

Reaction conditions are given in Fig. 1. Figure 2 shows that, over a 4-h period, about 50% of the rofecoxib is consumed. Note the similar increase in the major and minor product total peak areas over the same period. It is important to point out that even after the rofecoxib has been completely consumed, the furanone species persists. That is, the hydroxy-furanone **3** is not further oxidized to the dicarboxylic acid **4** under the reaction conditions. This observation is not consistent with oxidation mediated by peroxy radicals, in which rofecoxib would first be oxidized to the hydroxy-furanone, which would then be oxidized in a second step to the dicarboxylic acid **4** (1–3).

There is a marked pH dependence to the reaction rate. Figure 3 plots the % rofecoxib consumed during the first 5 min of the oxidation, as a function of the pH of the aqueous component of the reaction medium. Figure 3 shows that the reaction is negligible at pH 9 and 10, but rapidly accelerates near pH 11 and higher. At pH 12, all the rofecoxib is consumed within 25 min of the initiation of the oxidation.

Evidence of Base Catalyzed Enolate Ion Formation Under the Reaction Conditions

Rofecoxib (**1**) has a γ-lactone ring with a methylene carbon atom (designated as the C_5 position). The marked pH dependence shown in Fig. 3 led us to suspect that the oxidation reaction was being mediated by the rofecoxib enolate ion. At pH values near 11, hydroxide ion can remove a proton from one of the C–H bonds at the C_5 position to give the rofecoxib enolate ion. This reaction and the resulting resonance structures for the enolate ion (**5**) are shown in the upper portion of Scheme 2. Formaldehyde, a well-known electrophile, was added to the reaction mixture to probe for the presence of enolate ion (**5**). The resonance structures of **5** in Scheme 2 suggest that an addition reaction with formaldehyde might occur at either the C_5 or C_3 positions.

The upper chromatogram in Fig. 4 reflects 25 min of reaction time of 0.1 mg/mL rofecoxib in 50% acetonitrile/50% buffer (pH 11.0), to which one molar equivalent of formaldehyde was added. Two new species are formed

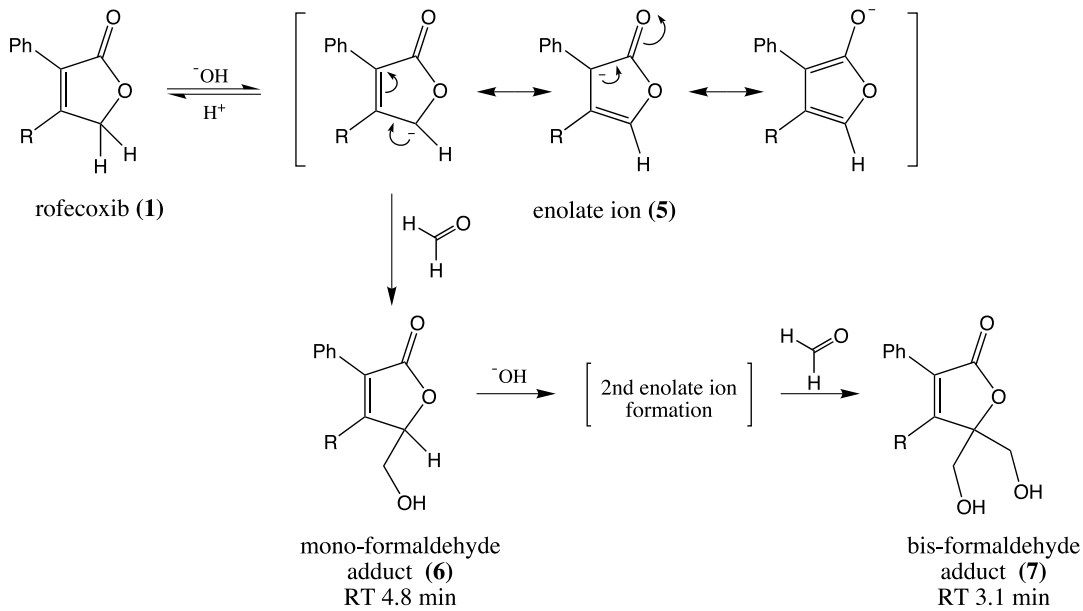

Scheme 2. Reaction of rofecoxib and formaldehyde at high pH.

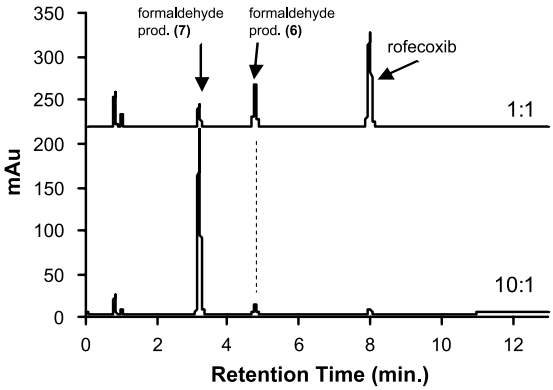

Fig. 4. Reaction conditions as in Fig. 1, except for the presence of formaldehyde at a 1:1 molar ratio with rofecoxib (upper) and a 10:1 molar ratio (lower). Chromatograms after 25 min reaction time. Note the new formaldehyde products species **6** and **7** at 3.1 and 4.8 min, respectively.

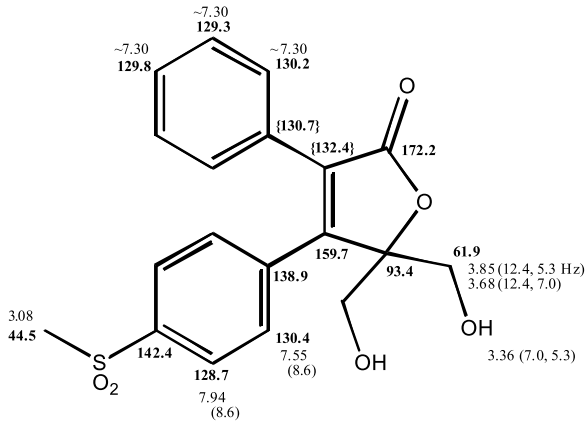

Fig. 5. Rofecoxib bis–formaldehyde adduct (**7**) structure as determined by NMR. Chemical shift assignments (CD_3CN; 25°C) are shown on the structure (carbon in bold, proton in normal font). Select proton–proton couplings (Hz) are given in parentheses. Braces denote carbon shifts that may be interchanged.

eluting near 3.1 and 4.8 min. When more formaldehyde is added, the species at 4.8 min disappears and only the species eluting at 3.1 min remains. The lower chromatogram in Fig. 4 is from a similar 25 min reaction time, except that a tenfold molar excess of formaldehyde was added. The species at 3.1 min dominates and the 4.8 min species is minor. Thus, rapid reaction with formaldehyde is demonstrated. The reaction with formaldehyde shows a similar pH dependence as that shown in Fig. 3. LC-MS analysis of the species eluting at 3.1 and 4.8 min indicates that these species have molecular weights which are 60 mass units and 30 mass units greater than rofecoxib, respectively. Each 30 mass unit gain is consistent with an addition reaction with formaldehyde. However, the location of each formaldehyde addition reaction could not be determined by LC-MS.

The species eluting near 3.1 min was therefore isolated and characterized by NMR. Based on the NMR analysis (proton 1D, HMQC, gHMBC, carbon 1D), 2 mol of formaldehyde had added to the C_5 position of the lactone ring, as shown in Fig. 5. The methylene was replaced with a quaternary carbon bearing two degenerate CH_2OH groups. The identity of the CH_2OH fragments was evident from the 61.9-ppm chemical shift of the carbon, the geminally coupled methylene protons (12.4 Hz between the resonances at 3.85 and 3.68 ppm) and the vicinally coupled (7.0 and 5.3 Hz), exchangeable proton at 3.36 ppm. The quaternary carbon was found to resonate at 93.4 ppm, 21.5 ppm downfield of the methylene carbon in rofecoxib. A downfield shift of this magnitude is within expectation for the added substituents. The methylene protons exhibited two-bond correlations to the 93.4-ppm carbon and three-bond correlations to the other, degenerate CH_2OH fragment. This is only possible when the two CH_2OH fragments are bonded to a common carbon as in the proposed structure. The location of the added CH_2OH fragments was further corroborated by three-bond correlations between each of the methylene protons (3.85, 3.68 ppm) and the lactone ring carbon at 159.7 ppm. The only carbon that was not observed via the long-range proton–carbon correlations of the gHMBC experiment was the lactone carbonyl carbon. It was necessary to run a direct observed carbon spectrum to obtain its chemical shift. All other carbon–proton correlations observed in the gHMBC experiment were found to be fully consistent with the structure and assignments shown in Fig. 5.

Thus, the structure determined in Fig. 5 shows that the C_5 position is uniquely favored in terms of reaction with an electrophile such as formaldehyde. Scheme 2 thus depicts our view of the formaldehyde product formation under the reaction conditions. Two sequential enolate ions form; in both cases, the addition reaction is favored at the C_5 position.

Determination of the Amount of Hydrogen Peroxide Liberated

Triphenylphosphine reacts rapidly and quantitatively with HOOH or ROOH to give 1 mol TPO for each mole of hydroperoxide reacted (10–12); an HPLC-based method for determination of hydrogen peroxide using TPP has been published previously (10). The HPLC methodology described here was used to determine the molar amount of hydrogen peroxide liberated during the oxidation reaction (conditions as in Fig. 1) at 0.5, 1, 2, and 4 h. At the detection wavelength of 203 nm, a simple preparation of TPO and TPP standard solutions shows that the molar response factors of TPO and

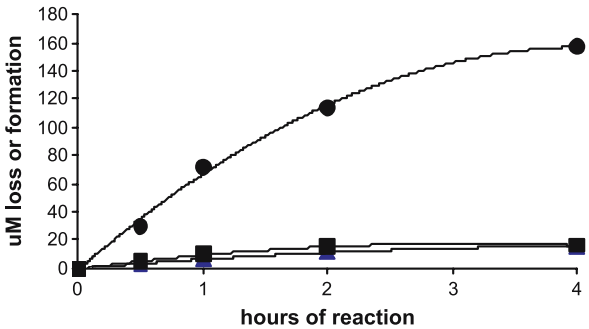

Fig. 6. Plot of micromolar rofecoxib lost (circles), micromolar furanone formed (triangles), and micromolar hydrogen peroxide generated (squares) over 4 h of the oxidation reaction time. Conditions as in Fig. 1. Note within experimental errors, furanone (**3**) and hydrogen peroxide are produced in a 1:1 molar ratio.

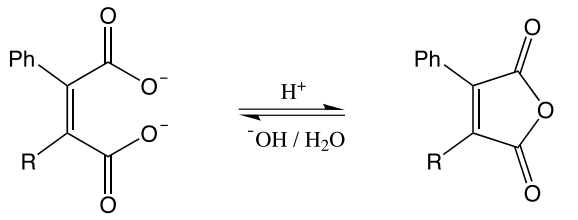

Scheme 3. Interconversion between anhydride (**8**) and dicarboxylate (**4**).

TPP are indistinguishable (data not shown). The TPO peak area is thus converted to TPO concentration using the TPP standard peak area and concentration. Figure 6 plots the molar amount of the rofecoxib lost, the molar amount of hydrogen peroxide detected, and the molar amount of the furanone species formed over the same time interval. The molar amount of rofecoxib lost is much greater than the molar amount of hydrogen peroxide liberated. Thus, the formation of the major dicarboxylate product (**4**) is not accompanied by the generation of a molar equivalent of hydrogen peroxide. In fact, Fig. 6 shows that the molar amount of hydrogen peroxide formed actually agrees very well with the molar amount of the *minor* hydroxy-furanone (**3**) oxidation product formed.

Evidence that the Rofecoxib Anhydride Species is Actually the Primary Oxidation Product

In the work of Mao *et al.*, the rofecoxib anhydride species was a significant peak in their chromatograms. It was pointed out that the presence of anhydride was due only to the fact that the samples were quenched with acid prior to HPLC injection. It was shown that acid quenching facilitates dicarboxylate ring closure to the anhydride prior to injection as shown in Scheme 3.

The authors noted that in the alkaline reaction medium, the ring-opened dicarboxylate (**4**) is the primary oxidation product. Consistent with this, the samples are not acid quenched in our work and there is no evidence of the rofecoxib anhydride species (**8**) in the chromatograms obtained under the typical reaction conditions (Fig. 1). If samples are first acid-quenched, however, a new peak eluting near 12.0 min appears. LC-MS data and a characteristic UV maximum near 350 nm as observed by Mao *et al.* confirm this species as anhydride (**8**).

When the water content of the oxidation reaction mixture is reduced and early timepoints are examined, low levels of the anhydride species (**8**) can be visualized in the chromatogram *without* acid quenching of the sample. It is worthwhile to note that the HPLC method conditions described here have been modified from Mao *et al.* (9) to optimize visualization of low levels of the anhydride (**8**). That is, the HPLC method utilized by Mao *et al.* used 0.1% phosphoric acid in the mobile phase, which leads to significant on-column interconversion between the anhydride (**8**) and the dicarboxylate (Scheme 3). The on-column interconversion makes low levels of the anhydride (**8**) more difficult to detect. We found that the rate of the interconversion between the dicarboxylate and the anhydride could be significantly decreased by changing the pH of the aqueous portion of the mobile phase to that of ambient $NaH_2PO_4 \cdot H_2O$ buffer (pH 4.6).

Figure 7 shows the 3- to 13-min elution region of three chromatograms, *none* of which has been acid-quenched prior to injection. With reaction conditions of 95% acetonitrile and 5% phosphate buffer at pH 12.0, the three chromatograms in Fig. 7 derive from injections at 0.65, 1.2, and 2.5 min. Note that *Y*-axis represents only 15 mAu compared to the 300 mAu scaling in Fig. 1. The rofecoxib anhydride (**8**) is clearly seen at 12.0 min in the earliest chromatograms. The UV spectrum and retention time match (compared to an acid-quenched sample) confirms it is the anyhydride (**8**). The intensity of the anhydride peak decreases as the amount of rofecoxib remaining decreases. As soon as the rofecoxib is

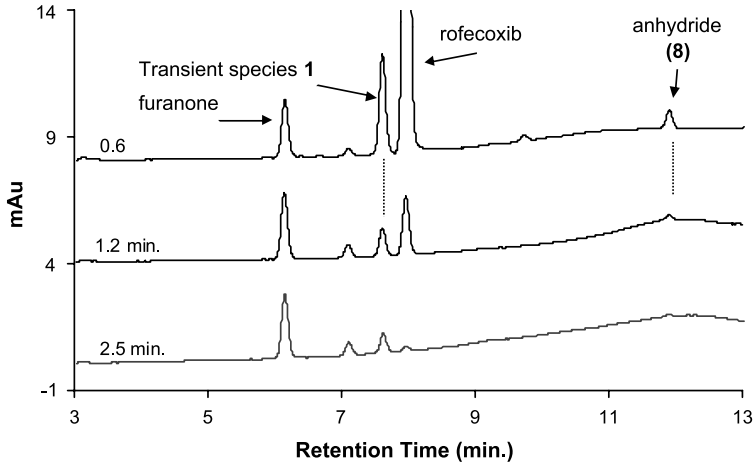

Fig. 7. Direct injections of oxidation reaction at 0.6, 1.2, and 2.5 min reaction time. Solvent composition is 95% acetonitrile, 5% phosphate buffer at pH 12.0. Note the presence of the rofecoxib anhydride (**8**) eluting near 12.0 min in earliest chromatograms. Note peak labeled transient species **1** also diminishes at longer times as rofecoxib is depleted.

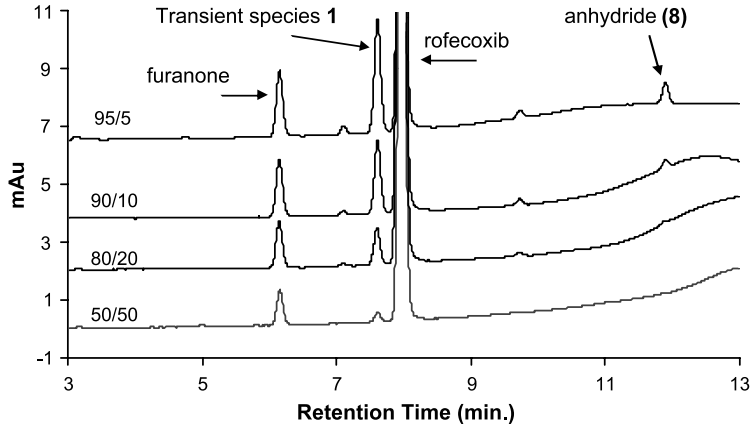

Fig. 8. Direct injections from oxidation reactions with 5, 10, 20, and 50% phosphate buffer at pH 12.0 (top to bottom). Reaction times are 0.6, 1.0, 1.7, and 4.0 min, respectively (top to bottom). Note rofecoxib anhydride (**8**) diminishes as phosphate buffer content is raised. Transient species **1** shows the same trend.

depleted, the anhydride (**8**) disappears from the chromatogram. These observations are consistent with the anhydride species (**8**) being formed directly from the rofecoxib oxidation, with subsequent rapid anhydride ring opening under the alkaline conditions to give the dicarboxylate (**4**).

As the phosphate buffer content in the reaction mixture is increased from 5 to 50%, the anhydride ring opening rate accelerates, whereas the rate of rofecoxib loss slows somewhat. This makes the transient accumulation of the anhydride increasingly difficult to detect in the chromatogram. This is shown in Fig. 8, which overlays early chromatograms from oxidation reactions at 5, 10, 20, and 50% phosphate buffer (pH 12.0) compositions. The anhydride (**8**) becomes progressively smaller at higher water levels. In the 20% buffer case, the anhydride (**8**) is barely visible, whereas at the standard conditions of 50% buffer the anhydride cannot be seen (lower chromatogram in Fig. 8). Thus at the standard 50% water levels, anhydride ring opening is faster than the rate at which the anhydride is being generated by the oxidation reaction. After completion of the studies shown in Figs. 7 and 8, the treatment of rofecoxib with *n*-butyl lithium in THF solvent open to air was reported (13). The primary product observed was the anhydride (**8**); no mechanistic investigation was reported (13). This finding is consistent with our conclusions regarding the anhydride (**8**) being the primary oxidation product in the acetonitrile/high pH water solvent system studied here.

Transient Formation of a Hydroperoxide of the Hydroxy-Furanone

Figures 7 and 8 also show the formation of a species designated "transient species **1**" eluting at 7.6 min just before rofecoxib (**1**). This species has the same behavior as the

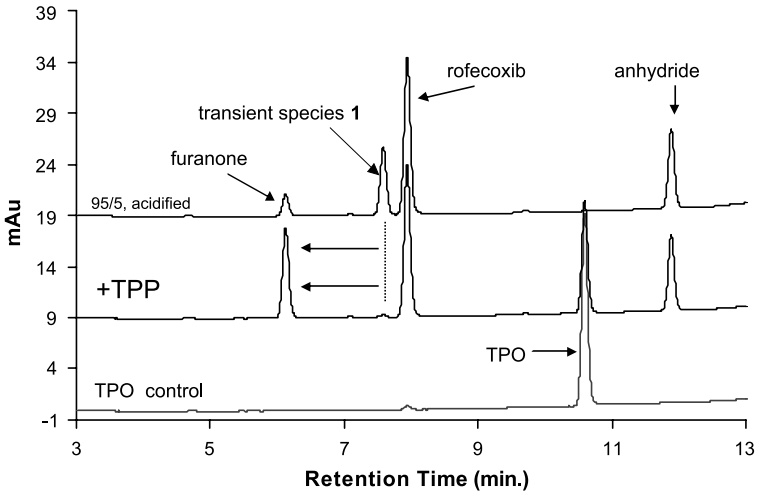

Fig. 9. Reaction of transient species **1** with TPP to form the furanone (**3**). Upper, acid quenched early reaction sample in 95% acetonitrile/5% phosphate buffer (pH 12.0). Middle, same sample with TPP added. Transient species **1** peak area is dramatically diminished, whereas furanone peak area is identically increased. Lower, dilute TPO sample to confirm TPO elution near 10.7 min. Note the anhydride (**8**) is more abundant here due to the acid quenching of the sample prior to injection (Scheme 3).

anhydride (**8**) in that it becomes smaller over time in Fig. 7, and decreases in abundance as the water level is raised in Fig. 8. This species can be shown to be a hydroperoxide by its reaction with TPP. Furthermore, after reaction with TPP, transient species **1** is in fact converted to the hydroxy-furanone (**3**). This is shown in Fig. 9. The upper chromatogram shows a sample similar to that described in the upper chromatograms in Fig. 7 [40 s reaction time in 95% acetonitrile/5% buffer (pH 12.0)], except that the sample was quenched with acid prior to injection. This stops both oxidation and any ring-opening hydrolytic reactions. All species in Fig. 9 are relatively stable under the acid-quenched conditions. Transient species **1** is noted and clearly evident in the upper chromatogram. The middle chromatogram is injected from the same quenched HPLC vial as the upper chromatogram, except that 40 μL of a 0.1 mg/mL solution of TPP was added to the HPLC vial 15 min prior to injection. Transient species **1** peak is dramatically reduced, whereas the furanone peak is similarly increased in intensity. The peak area gain of the hydroxy-furanone is quantitatively equal to the peak area lost from transient species **1**. triphenylphosphine reacts with organic hydroperoxides, R-OOH, converting them to the corresponding alcohol (R-OH) with retention of stereochemistry at the carbon atom (11,12). The lower chromatogram is from injection of a 40-μM solution of TPO. This shows that the peak near 10.6 min is in fact the TPO formed from the TPP reaction with Transient species 1 (TPP does not elute in the retention time window shown in Fig. 9). Figure 9 suggests the assignments shown in Scheme 4.

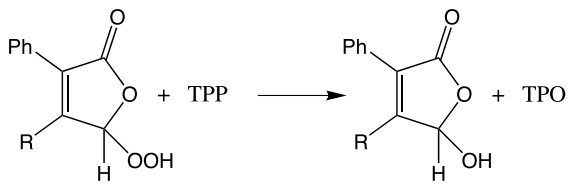

transient hydroperoxide (**9**) ("transient species **1**")

furanone (**3**)

Scheme 4. Reaction of triphenylphosphine with transient species **1**.

DISCUSSION

Reaction of Carbanions With Molecular Oxygen

The reaction of carbanions with molecular oxygen has been studied in the context of base catalyzed oxidation and has been reviewed (14). Treatment of substrates with weakly acidic C–H bonds such as aliphatic nitro compounds (15), triphenylmethane (16), ketones and esters (17), aryl propenes (18), and nitriles (19) with alkoxide bases was found to yield carbanions that could readily react with dissolved oxygen. Scheme 5 depicts the ionization step and the subsequent reaction with oxygen.

The first product is a hydroperoxide anion. The simple "one-step" addition of the carbanion to molecular oxygen to directly give the hydroperoxide anion has been proposed (17), but others point out that such a process would be a violation of the spin conservation rule (15,16,18). The bracketed or "caged" species in Scheme 5 addresses that concern (in which oxygen is proposed to accept an electron

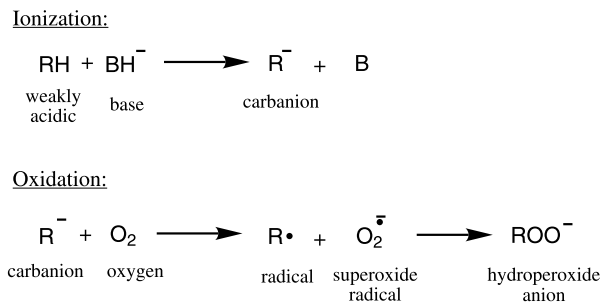

Scheme 5. Reaction of carbanions with molecular oxygen.

from the carbanion to form a carbon radical and superoxide radical, followed by spin inversion and combination to give the hydroperoxide anion product). In either case, the primary product is the hydroperoxide anion. Thus, the new C–O bond formation depicted in Scheme 5 can proceed rapidly, because there is no C–H bond hydrogen atom abstraction by peroxy radical, which is the rate limiting process in the free radical chain oxidation pathway.

Mechanism for the High pH Rofecoxib Oxidation

Under the typical high pH reaction conditions, when increasing levels of formaldehyde are added we observe that the yields of the oxidation products **3** and **4** progressively decrease as the formaldehyde addition products increase (Figs. 1 and 4). Thus, it is clear both oxygen and formaldehyde are competing for the enolate ion (**5**). We propose that the enolate ion (**5**) and its contributing resonance structures (Scheme 2) provide sufficient "carbanion" character to facilitate reaction with molecular oxygen, as shown in Scheme 5. This type of reaction with oxygen would explain the dramatic pH effect in Fig. 3 as well as the very rapid rate of oxidation, because C–H bond abstraction by peroxy radicals is not involved. In addition, any proposed mechanism for the high pH oxidation of rofecoxib must also account for five other important observations described as follows:

(1) Rofecoxib anhydride (**8**) is a primary product of the oxidation reaction; hydrolysis of the anhydride to the observed dicarboxylate (**4**) is a secondary reaction.

(2) Formation of **8** proceeds without the liberation of hydrogen peroxide.

(3) The mechanistic routes to the hydroxy-furanone (**3**) and the dicarboxylate (**4**) cannot be sequential, but rather must be divergent to explain the fact that the hydroxy-furanone (**3**), once formed, is stable under the reaction conditions.

(4) The molar amount of hydrogen peroxide liberated corresponds to the molar amount of the minor furanone (**3**) product formed.

(5) There is transient formation of a hydroperoxide analog of the hydroxy-furanone (**3**).

The mechanism we propose, which accounts for all these observations, is shown in Scheme 6.

At pH values near 11, hydroxide ion facilitates formation of the enolate ion (**5**). The enolate ion (**5**) donates an electron to molecular oxygen; the resulting rofecoxib radical

and superoxide radical rapidly combine selectively at C_5 to form the new hydroperoxide anion group at that position. Protonation of the hydroperoxide anion gives the transient hydroperoxide (**9**) in Scheme 6. This species is "transient species **1**" in Figs. 7, 8, 9, and in Scheme 4. It is interesting to note that the C_5 position is favored for both the "two-electron" formaldehyde addition reaction (Scheme 2), as well as the combination reaction of the rofecoxib radical and superoxide radical.

There are two distinct pathways available to the transient hydroperoxide (**9**). The major pathway is the formation of a second enolate ion, as was demonstrated in the presence of formaldehyde. The second enolate ion formation is shown in Scheme 6 as species **10**. The enolate ion (**10**) is proposed to undergo a decomposition in which the electron density is drawn to the C–O bond of the hydroperoxide group, and creates a new carbon–oxygen double bond. This requires the concomitant heterolytic cleavage of the peroxide bond and the liberation of hydroxide ion. This decomposition is depicted by the arrows shown in right-hand enolate ion (**10**) structure in Scheme 6. A similar decomposition has been proposed to explain the differences in product distributions in base catalyzed oxidation of primary and secondary nitriles (14,19). In Scheme 6, the product of this unique decomposition is the rofecoxib anhydride (**8**). The anhydride (**8**) is rapidly hydrolyzed under the alkaline conditions to the observed dicaboxylate product (**4**).

A minor pathway for the transient hydroperoxide (**9**) is ring opening by hydroxide ion, which leads to the unstable species (**11**) in Scheme 6. Species **11** has both an alcohol and a hydroperoxide group on C_5, which facilitates rapid rearrangement to the aldehyde and concomitant elimination of hydrogen peroxide. This gives the hydroxy-furanone (**3**) in the open form that would be in rapid equilibrium with the closed ring form. We are not certain which form of **3** dominates under the alkaline pH conditions, but it does not impact Scheme 6 in either case. Scheme 6 thus accounts for all critical observations. The pathway to the furanone (**3**) and the dicarboxylate (**4**) is not stepwise, in that they are two different routes of decomposition of the transient hydroper-

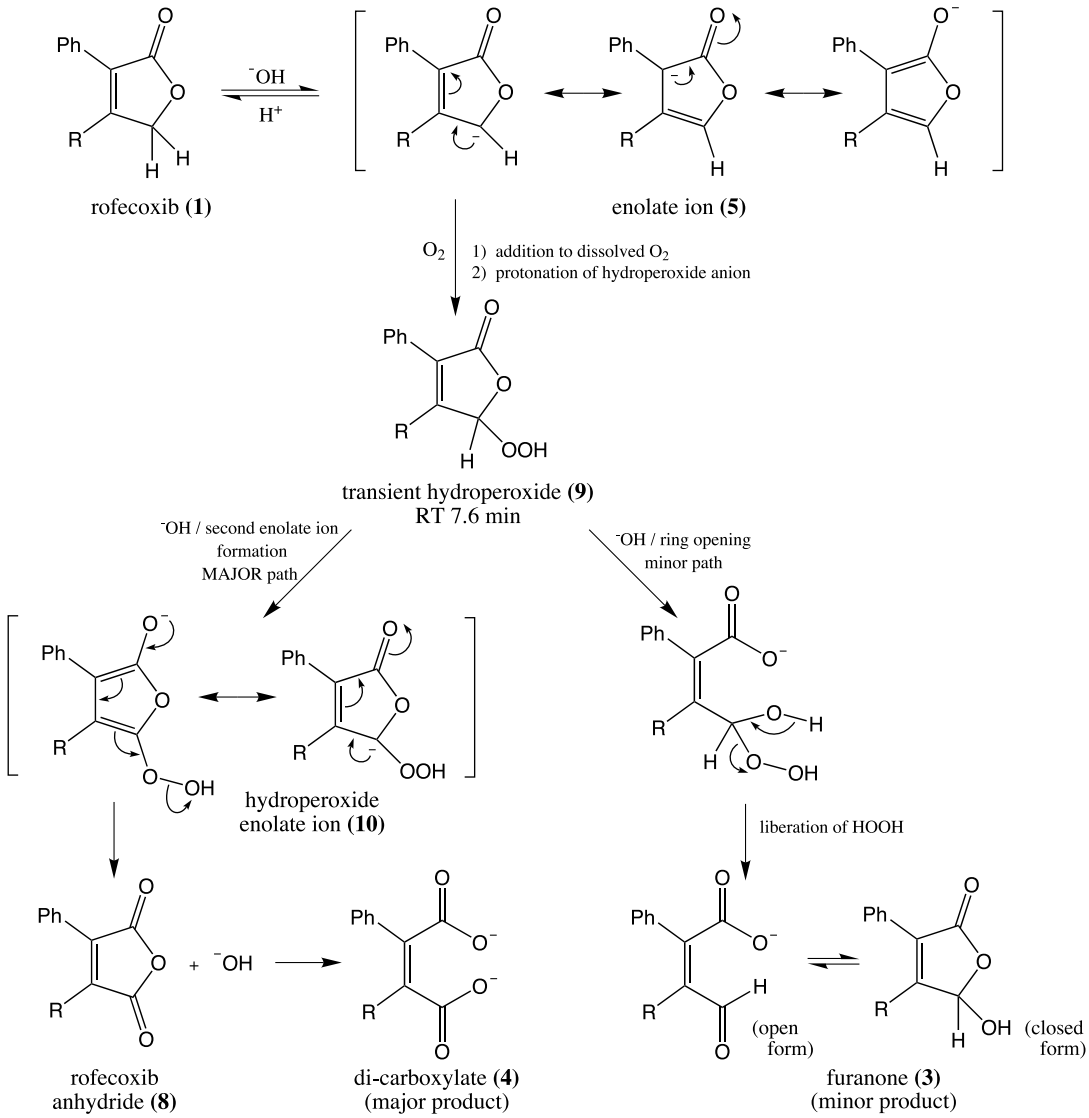

Scheme 6. Mechanism of rofecoxib oxidation under high pH conditions.

oxide (**9**). The major pathway yields the anhydride (**8**) without liberation of hydrogen peroxide, whereas the minor pathway that leads to the furanone (**3**) must liberate a molar equivalent of hydrogen peroxide.

The stability of the hydroxy-furanone (**3**) under the alkaline reaction conditions is worthy of comment. In the closed ring form of the hydroxy-furanone (**3**), enolate ion formation seems possible. We can only suggest that if the enolate ion does form, the resulting "carbanion character" of C_5 must not be sufficient to give reaction with molecular oxygen. In that context, it is interesting to note that there is also no significant reaction of the hydroperoxide enolate ion (**10**) with dissolved oxygen. Addition of **10** to oxygen (at the C_5 position) would result in a dihydroperoxide or related decomposition product, for which we find no chromatographic evidence. In both **10** and the enolate ion of the hydroxy-furanone (**3**), there is an additional carbon–oxygen bond at C_5 compared to the enolate ion (**5**). We speculate this has the net effect of decreasing the electron density at C_5 compared to **5**.

In Scheme 6, there is no requirement for opening of the γ-lactone ring of rofecoxib (**1**) prior to the oxidation. In Scheme 6, the γ-lactone ring is opened only as a minor pathway in species **9**. In our view, the γ-lactone ring of **1** is relatively stable under the basic reaction conditions. Direct injections of the alkaline reaction mixtures have never shown any rofecoxib peak area shift or distortion to earlier retention times, which would be expected from the presence of some fraction of the alcohol (**2**). The bis-formaldehyde adduct (**7**) peak shape also does not change over time in the alkaline reaction medium, suggesting the lactone ring of this species is similarly stable toward hydrolysis.

Potential for Base Catalyzed Oxidation During Forced Degradation Studies

Rofecoxib serves as a case study highlighting that certain structural classes of compounds may have the potential for an "alternative" oxidation pathway at alkaline pH values. If a compound can be ionized as in Scheme 5, then new C–O bond formation may proceed as shown in Schemes 5 and 6. This type of oxidation can proceed rapidly because hydrogen atom abstraction by peroxy radicals is not involved. One scenario in which the alkaline pH oxidation described here might be encountered is during forced degradation studies. Forced degradation studies often probe for hydrolytic instability by dissolving the drug in solutions at pH values of 10–13 (20). Under these conditions, rofecoxib (**1**) would rapidly degrade by the subject oxidation, rather than by hydrolysis. Ketorolac tromethamine was also shown to oxidize as in Scheme 5, in solution at pH values above 8 (6). These cases serve as a general reminder that for drug substances that show increasing instability at more alkaline pH values, complete structural characterization of all degradation products being formed may be needed to distinguish hydrolytic degradation pathways from the oxidative degradation pathway shown in Scheme 5.

CONCLUSIONS

The mechanism of the oxidation of rofecoxib under high pH solution conditions was investigated. The primary product of the oxidation reaction was shown to be the rofecoxib anhydride (**8**), which is rapidly hydrolyzed under the alkaline reaction conditions to give the observed dicarboxylate (**4**) as the major product. The reaction was shown to be a base catalyzed oxidation, in which the rofecoxib enolate ion (**5**) is formed as an intermediate. The enolate ion (**5**) undergoes an anionic reaction with oxygen as shown in Scheme 5, in which an electron is transferred to oxygen and the resulting radical species combine selectively at C_5. This mechanism explains the rapid oxidation rate and the observed pH dependence. Peroxy radicals are not involved in the oxidation. The oxygen reaction at C_5 gives a key transient hydroperoxide (**9**), from which there is a major and a minor reaction pathway. The major pathway leads to the rofecoxib anhydride (**8**), and proceeds through a second enolate ion formation and subsequent decomposition in which the hydroperoxide bond is heterolytically cleaved. The minor route of reaction of hydroperoxide (**9**) involves hydrolysis of the γ-lactone ring, followed by facile liberation of hydrogen peroxide to yield the hydroxy-furanone (**3**).

ACKNOWLEDGMENTS

The authors would like to thank Dr. Bill Bowen for useful discussions and ideas. We gratefully acknowledge Merck and Co. for funding this work.

REFERENCES

1. S. W. Hovorka and C. Schoneich. Oxidative degradation of pharmaceuticals: theory, mechanisms and inhibition. *J. Pharm. Sci.* **90**:253–269 (2001).
2. D. M. Johnson and L. C. Gu. Autoxidation and antioxidants. In J. Swarbrick and J. C. Boyland (eds.), *Encyclopedia of Pharmaceutical Technology*, Marcel Dekker, New York, 1988, pp. 415–449.
3. R. A. Sheldon and J. K. Kochi. Metal—catalyzed oxidations of organic compounds in the liquid phase: a mechanistic approach. In W. G. Frankenburg (ed.), *Advances in Catalysis*, Academic Press, New York, 1976, pp. 273–413.
4. J. March. *Advanced Organic Chemistry: Reactions, Mechanisms, and Structure*, 4th ed. John Wiley and Sons, New York, 1992, pp. 198–1202.
5. K. J. Hartauer, G. N. Arbuthnot, S. W. Baertschi, R. A. Johnson, W. D. Luke, N. G. Pearson, E. C. Rickard, C. A. Tingle, P. K. S. Tsang, and R. E. Wiens. Influence of peroxide impurities in povidone and crospovidone on the stability of raloxifene hydrochloride in tablets: identification and control of an oxidative degradation product. *Pharm. Dev. Technol.* **5**(3): 303–310 (2000).
6. L. Gu, H. S. Chiang, and A. Becker. Kinetics and mechanisms of the autoxidation of ketorolac tromethamine in aqueous solution. *Int. J. Pharm.* **41**:95–104 (1988).
7. E. Lemp, C. Valencia, and A. L. Zanocco. Solvent effects on reactions of singlet molecular oxygen with antimalarial drugs. *J. Photochem. Photobiol., A* **168**:91–96 (2004).
8. F. Vargas, M. V. Hisbeth, and J. K. Rojas. Photolysis and photosensitized degradation of the diuretic drug acetazolamide. *J. Photochem. Photobiol., A* **118**:19–23 (1998).
9. B. Mao, A. Abrahim, Z. Ge, D. K. Ellison, R. Hartman, S. V. Prabhu, R. A. Reamer, and J. Wyvratt. Examination of rofecoxib solution decomposition under alkaline and photolytic stress conditions. *J. Pharm. Biomed. Anal.* **28**:1101–1113 (2002).
10. T. Nakamura and H. Maeda. A simple assay for lipid hydroperoxides based on triphenylphosphine oxidation and high performance liquid chromatography. *Lipids* **26**:765–768 (1991).

11. A. G. Rowley. Conversions via oxygenation. In J. I. G. Cadogan (ed.), *Organophosphorous Reagents in Organic Synthesis*, Academic Press, New York, 1979, pp. 318–327.
12. H. Yin and N. A. Porter. Specificity of the ferrous oxidation of xylenol orange assay: analysis of the autoxidation products of cholesteryl arachidonate. *Anal. Biochem.* **313**:319–326 (2003).
13. L. R. Reddy and E. J. Corey. Facile air oxidation of the conjugate base of rofecoxib, a possible contributor to chronic human toxicity. *Tetrahedron Lett.* **46**:927–929 (2005).
14. G. Sosnovsky and E. H. Zaret. Base catalyzed autoxidation. In D. Swern (ed.), *Organic Peroxides*, J. Wiley and Sons, New York, 1971, pp. 517–560.
15. G. A. Russell. The autoxidation of 2-nitropropane in basic solution. *J. Am. Chem. Soc.* **76**:1595–1600 (1954).
16. G. A. Russell and A. G. Bemis. The oxidation of carbanions: I. Oxidation of triaryl carbanions and other tertiary carbanions. *J. Am. Chem. Soc.* **88**:5491–5497 (1966).
17. H. R. Gersmann and A. F. Bickel. Autoxidation of ketones and esters in basic solution. *J. Chem. Soc., (B)* **11**:2230–2237 (1971).
18. D. H. R. Barton and D.W. Jones. Autoxidation in basic media. Part IV. Hydrocarbon autoxidation. *J. Chem. Soc.* 3563–3570 (1965).
19. H. G. Aurich. Zum Mechanismus Der Autoxydation Von Nitrilen In Gegenwart Von Basen. *Tetrahedron Lett.* **12**:657–658 (1964).
20. K. M. Alasante, L. Martin and S. W. Baertschi. A stress testing benchmarking study. *Pharm. Technol.* (**Feb 02**):60–72 (2003).